JOC The Journal of Organic Chemistry

Note

pubs.acs.org/joc

Spectroscopic and Structural Characterization of the CyNHC Adduct of B_2pin_2 in Solution and in the Solid State

Christian Kleeberg,[†] Andrew G. Crawford,[†] Andrei S. Batsanov,[†] Paul Hodgkinson,*[,†] David C. Apperley,[†] Man Sing Cheung,[‡] Zhenyang Lin,*[,‡] and Todd B. Marder*[,†]

[†]Department of Chemistry, Durham University, South Road, Durham, DH1 3LE, United Kingdom

[‡]Department of Chemistry, The Hong Kong University of Science and Technology, Clear Water Bay, Kowloon, Hong Kong, China

Supporting Information

ABSTRACT: The Lewis base adduct of B_2pin_2 and the NHC (1,3-bis(cyclohexyl)imidazol-2-ylidene), which was proposed to act as a source of nucleophilic boryl groups in the β-borylation of α,β-unsaturated ketones, has been isolated, and its solid state structure and solution behavior was studied. In solution, the binding is weak, and NMR spectroscopy reveals a rapid exchange of the NHC between the two boron centers. DFT calculations reveal that the exchange involves dissociation and reassociation of NHC rather than an intramolecular process.

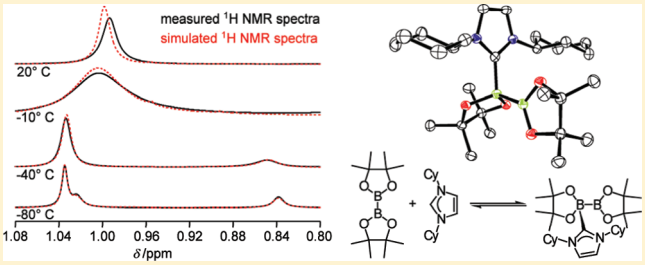

Sp^2–sp^3 diboron compounds have been reported previously[1] and were postulated as intermediates in both transition metal and organo-catalyzed borylation reactions.[2] However, their reactivity has neither been studied in great detail, nor have they been used explicitly as reagents until recently.[3] Hoveyda et al. postulated that a neutral, intermolecular Lewis base adduct of B_2pin_2 (**1**, pin = $OCMe_2CMe_2O$) and the *N*-heterocyclic carbene CyNHC (**2**, 1,3-bis(cyclohexyl)imidazol-2-ylidene) acts as a boron nucleophile in the NHC-catalyzed β-borylation of α,β-unsaturated ketones[4] (Scheme 1), a novel organo-

Scheme 1. NHC-Catalyzed Borylation Reported by Hoveyda et al.

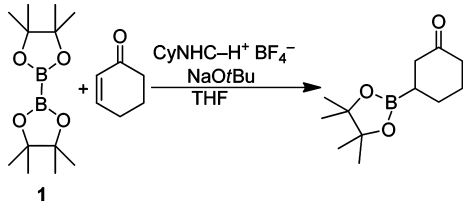

1

catalytic process distinct from those previously reported involving Cu-catalysis.[2a,5] While DFT calculations suggested the existence of this adduct, Hoveyda et al. initially reported only ^{11}B NMR signals at 4.5 and 6.3 ppm as experimental data supporting its formation.[4]

The initial ^{11}B NMR data were suspicious, as they are not in agreement with our own studies on related neutral adducts of $B_2(O_2C_6H_4)_2$ and $B_2(S_2C_6H_4)_2$[1b,c] or ionic sp^2–sp^3 adducts of **1**[6] or with the data reported for the intramolecular adduct pinacolato diisopropanolaminato diboron.[3] Generally, two well-separated signals are observed at >20 ppm (sp^2-B) and <10 ppm (sp^3-B).[7] The report of this intriguing adduct triggered us to investigate in detail its structural and spectroscopic properties in solution and in the solid state.

As suggested by Hoveyda et al., the highly Lewis basic carbene **2** does react with **1**, cleanly forming the intermolecular adduct **3** (Scheme 2, Figure 1), which can be crystallized from PhMe as a 1:1 solvate.

Scheme 2. Formation of the sp^2–sp^3 Diboron Compound 3

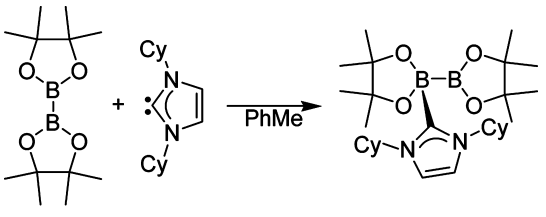

1 **2** **3**

For comparison, we redetermined the crystal structure of **1** at low temperature, as the previously reported[8a] one appears to contain unresolved disorder resulting in inaccuracies in key bond lengths.[8b,9] The B–B distance in **3** is 0.039 Å longer than in the low temperature structure of **1** (1.704(1) Å),[9] as expected from the change in hybridization of one of the boron atoms.[1b,c,3] The sp^3 boron center B2 exhibits a distorted tetrahedral geometry, whereas B1 is virtually planar (maximum deviation from the B1, B2, O1, O2 plane: 0.009(2) Å), with B1–O1 and B1–O2 distances comparable to those in related

Received: November 3, 2011
Published: November 29, 2011

   dx.doi.org/10.1021/jo202127c | *J. Org. Chem.* 2012, 77, 785–789

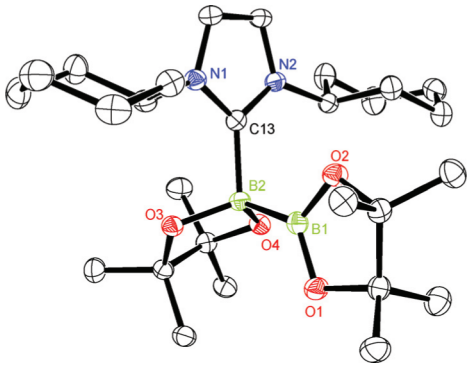

Figure 1. Molecular structure of **3** (in **3**·PhMe). Thermal ellipsoids are drawn at the 50% probability level; hydrogen atoms and solvent are omitted for clarity. Selected bond lengths (Å) and angles (°): B1−B2 1.743(2), O1−B1 1.379(2), O2−B1 1.386(2), O3−B2 1.490(2), O4−B2 1.483(2), C13−B2 1.673(2), O3−B2−O4 104.6(1), O3−B2−C13 107.6(1), O4−B2−C13 111.7(1), O3−B2−B1 116.6(1), O4−B2−B1 111.1(1), C13−B2−B1 105.4(1).

arylboronates.[10] The B2−C13 distance of 1.673(2) Å is similar to that of 1.683(6) Å found in a triethylborane *i*PrNHC (1,3-bis(isopropyl)imidazol-2-ylidene) adduct.[11,12]

The experimental solid-state structure of **3** is in good agreement with that calculated by DFT methods in the gas phase by Hoveyda et al.[4] Using the simplified model $(MeNHC)B_2pin_2$ (MeNHC = 1,3-bis(methyl)imidazol-2-ylidene), we also obtained a very similar optimized geometry (B3LYP/6-31G*; B1−B2 1.734 Å, O1−B1 1.419 Å, O2−B1 1.407 Å, O3−B2 1.483 Å, O4−B2 1.490 Å, C13−B2 1.671 Å; gas phase).

Having verified that adduct **3** can be formed, its ^{11}B NMR spectrum deserves closer attention, as the data reported initially by Hoveyda et al. are not in agreement with expected values (vide supra). The variable temperature ^{11}B NMR spectra give

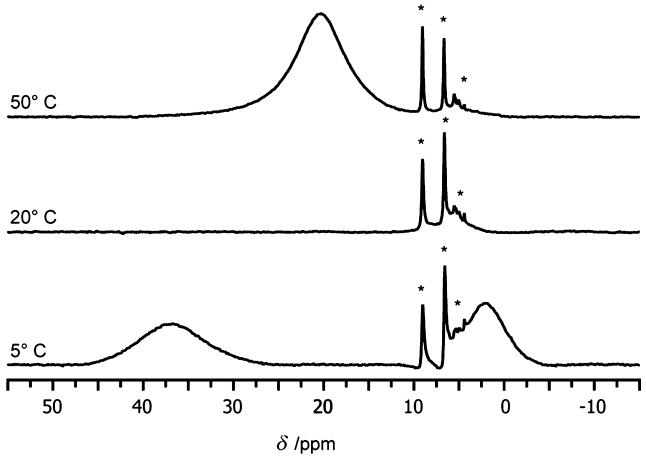

Figure 2. Selected variable temperature $^{11}B\{^1H\}$ NMR (160 MHz) spectra of **3** in THF-d_8 (∗ impurity, see text). The data were processed using back linear prediction (LP) of the initial 11 data points and an exponential window function (10 Hz).

evidence for the dynamic behavior of **3** in solution (Figure 2). At 50 °C, one averaged ^{11}B signal at 20.4 ppm is detected. At 20 °C, no signal is detected because of the broadening of the signal close to the coalescence temperature and the applied data processing (vide infra). Decreasing the temperature to 5 °C leads to the appearance of two signals, resulting from the tetrahedral (2.4 ppm) and the trigonal-planar (37.2 ppm) boron sites. This is in agreement with isotropic chemical shifts of 36 and 2 ppm that we observed in the solid-state ^{11}B NMR spectrum[9] and with the corrected solution NMR data reported[4b] by Hoveyda et al. while this work was in progress.

Because of the quadrupolar nature of the ^{11}B nucleus (I = 3/2, Q = 4.059 × 10^{26} m^2, N.A. = 80.1%), it is subject to quadrupolar coupling, and the quadrupolar relaxation pathways typically results in very short transverse relaxation times (T_2), and hence broad line widths. The observation of such broad signals is further complicated by the presence of borosilicate glass in standard NMR probe heads and NMR tubes. Therefore, a very broad background signal (ca. 100 ppm

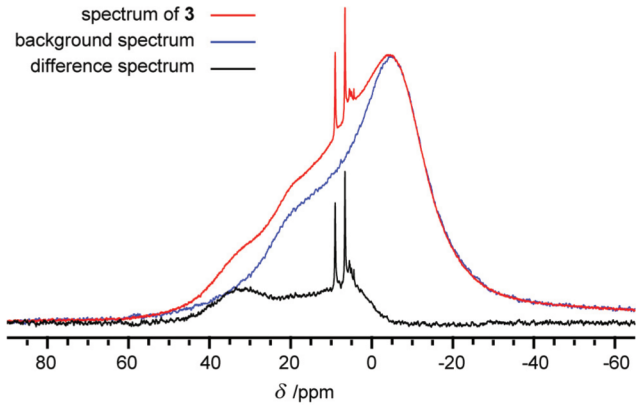

Figure 3. $^{11}B\{^1H\}$ NMR (160 MHz) spectrum of **3** in THF-d_8 at 20 °C, a background spectrum under virtually identical conditions and the difference spectrum. A 10 Hz exponential window function was included in the processing.

wide) arising from the glass must be suppressed (Figure 3). This is typically done by deletion of the first few data points of the FID, followed by reconstruction using back linear prediction (LP). This suppresses especially broad signals from the glass that decay very quickly, but also *any genuinely broad signals* resulting from chemical exchange or fast T_2 relaxation of the sample.

An alternative approach that suppresses only the boron signal from the glass is to subtract a background spectrum measured under identical conditions. Using this method, the spectrum of **3**, at 20 °C, shows a very broad, double humped signal at ca. 20 ppm, indicative of being close to the coalescence temperature for the dynamic process (Figure 3).

Hoveyda et al. proposed the in situ formation of **3** on the basis of ^{11}B NMR spectroscopic data and DFT calculations. Sharp ^{11}B NMR signals at 6.3 and 4.5 ppm (solvent not reported) in a mixture of **1** and **2** were initially assigned to **3**[4] and likely correspond to the unusually sharp signals between 10 and 4 ppm observed here (major signals at 9.0 and 6.6 ppm at 20 °C). These signals, which clearly result from impurities or decomposition products in the sample, were observed repeatedly to a varying extent despite taking every precaution to ensure the purity of the analyzed sample of **3** and the NMR solvent.[13] The integrated intensity of these signals is small compared to those of **3** (integral ratio ^{11}B NMR at 20 °C: 100:8) and is consistent with a signal in the ^1H NMR spectrum (integral ratio: 100:6 at 20 °C, Figure 4). Additionally, the chemical shifts and peak widths of these signals contradict all expectations for an sp^2−sp^3 diboron compound (vide supra), in

dx.doi.org/10.1021/jo202127c | J. Org. Chem. 2012, 77, 785−789

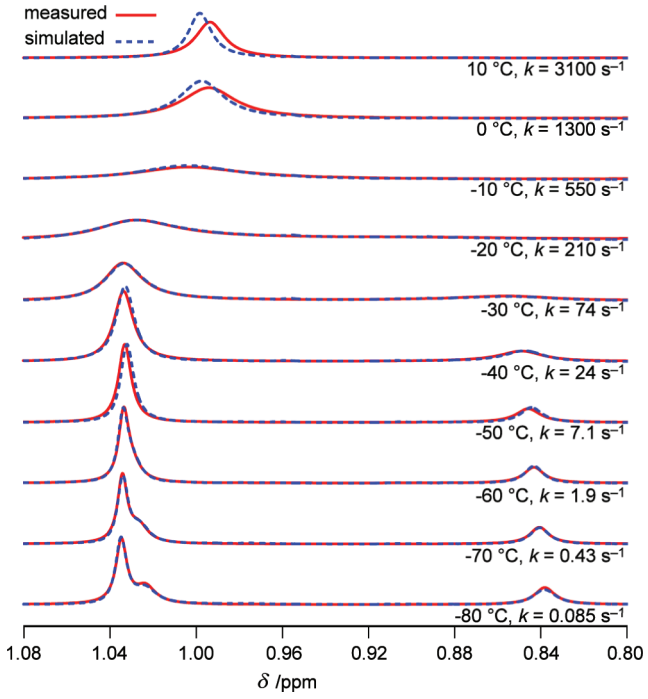

Figure 4. Details of selected variable temperature ^{1}H NMR (500 MHz) spectra of **3** in THF-d_8 and simulated spectra. The exchange rates at each temperature for complexation/decomplexation, k, calculated from the fitted activation parameters are shown.

contrast with the chemical shifts we observe in both solution-state and solid-state ^{11}B NMR spectra of **3**. They are, however, typical in position and line width of highly symmetric, four-coordinate boron (i.e., tetrahedral borate with a minimal electric field gradient at the nucleus) suggesting a species such as $[Bpin_2]^-$. Thus, adopting a procedure reported for related alkali metal salts of $[Bpin_2]^-$,[9,14] we synthesized and characterized spectroscopically and structurally $[nBu_4P]^+[Bpin_2]^-$. The observed ^{11}B NMR chemical shift of 8.6 ppm in THF-d_8 suggests, considering the different counterions and the different dielectric constant of the solvent, that the borate $[Bpin_2]^-$ is indeed a decomposition product of the adduct **3**, although the nature of the corresponding cation is as yet unknown.

As a quantitative study of **3** in solution via ^{11}B NMR is difficult, ^{1}H NMR was used to obtain kinetic data of its dynamic behavior. Figure 4 shows the signals from the pinacolate methyl groups as a function of temperature. The spectrum at −80 °C is consistent with the solid state-structure of **3** (Figure 1). There are three resolved methyl signals (δ = 1.04, 1.03, 0.84 ppm) in a ratio of 12:6:6. The two smaller signals correspond to the four methyl groups at the tetrahedral boron atom, two facing toward the CyNHC moiety and the other two facing away from it. Only one signal is observed for the pinacolate moiety at the trigonal-planar boron atom, implying that rotation around the B−B bond is fast even at −80 °C.[9] Increasing the temperature, e.g., to −40 °C, leads to a broadening of the signals and small shifts until only one signal at an averaged chemical shift is observed (δ = 1.00 ppm at 20 °C), implying equivalence of the pinacolate moieties on the NMR time scale.

Figure 4 also shows the result of modeling this portion of ^{1}H VT NMR spectra in terms of an exchange process that interconverts the pinacolate moieties. The exchange rate constant, k, is assumed to follow the Eyring equation: $k = (k_bT/h)\exp(-\Delta G^{\ddagger}/RT)$. The set of spectra from −80 to 10 °C were simultaneously fit to a single set of parameters using the protocol described in the Supporting Information.[9] The fitting is very satisfactory given the assumptions involved, particularly the linear extrapolatation of the temperature dependence of the chemical shifts from the low temperature spectra over the full temperature range. However, significant deviations are observed at the higher temperatures, which are consistent with a partial dissociation of **3**, i.e., the single resonance frequency is a weighted average of the Me shifts in adduct **3** and free **2**. The degree of dissociation, i.e., [**3**]/[**2**], is estimated very approximately to be 5% at 20 °C, on the basis of the deviation between the expected and observed mean shifts and a measurement of the Me shift of free **2** (1.18 ppm at 20 °C). This estimate is extremely sensitive to the extrapolation of the shift values noted above. The fitted enthalpy and entropy of activation for the exchange process are: $\Delta H^{\ddagger}$ = 51.1 ± 0.6 kJ mol^{-1} and $\Delta S^{\ddagger}$ = 2.6 ± 2.4 J K^{-1} mol^{-1}.

The spectral noise level is too low to limit the accuracy of the results, and so the 2σ error bars quoted are based on the rms deviation between fitted and experimental spectra. The correlation coefficient between the entropy and enthalpy parameters is extremely high (>0.999), so these individual values should be treated with caution; the decomposition into $\Delta H^{\ddagger}$ and $\Delta S^{\ddagger}$ contributions is much less reliable than the $\Delta G^{\ddagger}$ value for this type of band shape analysis.[15a] $\Delta G^{\ddagger}_{298}$ is calculated to be 50.3 kJ mol^{-1}. While the ^{11}B NMR spectra are unsuitable for detailed line shape analysis, $\Delta G^{\ddagger}_{298}$ is estimated to be ca. 50 kJ mol^{-1} on the basis of the signal separation at low temperature (5 °C) and the coalescence temperature (25 °C),[15] in excellent agreement with the value obtained via analysis of the ^{1}H NMR spectra.

To understand better the nature of the dynamic exchange process, DFT calculations were performed on the simplified

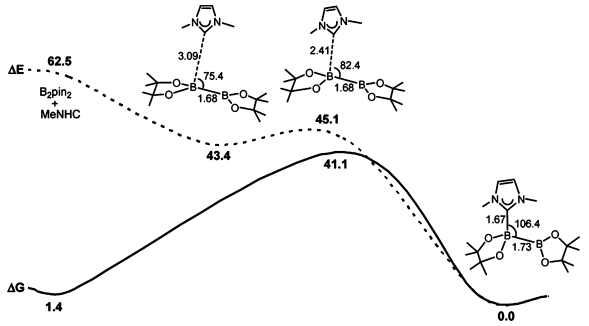

Figure 5. Energy profiles calculated for the association process of NHC and B_2pin_2. Relative free energies (ΔG_{298}) and electronic energies (ΔE_{298}, dotted line) are given in kJ mol^{-1}, and selected bond lengths and bond angles are given in Å and °, respectively.

model adduct (MeNHC)B_2pin_2.[9] Figure 5 shows the energy profiles calculated for the association process of NHC and B_2pin_2. NHC and B_2pin_2 form a complex of van der Waals type, from which overcoming a very small barrier leads to the formation of the adduct (MeNHC)B_2pin_2. The small barrier is related to the pyramidalization process at the boron center to which the NHC is bonded. From Figure 5, it can be seen that a transition state corresponding to an intramolecular exchange of the NHC between the two boron centers could not be located.

dx.doi.org/10.1021/jo202127c | J. Org. Chem. 2012, 77, 785−789

Instead, the profiles suggest a dissociation−reassociation mechanism for the dynamic exchange process.

The computed kinetic values for the adduct dissociation in the gas phase are $\Delta H^{\ddagger}_{298}$ = 41.8 kJ mol^{-1}, $\Delta S^{\ddagger}_{298}$ = 2.5 J K^{-1} mol^{-1}, and $\Delta G^{\ddagger}_{298}$ = 41.1 kJ mol^{-1}, in good agreement with the experimental values. The computed thermodynamic values for adduct formation in the gas phase are ΔH_{298} = −57.4 kJ mol^{-1}, ΔS_{298} = −188.4 J K^{-1} mol^{-1}, and ΔG_{298} = −1.4 kJ mol^{-1}. The very small value of ΔG_{298} suggests that the (MeNHC)B_2pin_2 adduct is relatively weakly bound. Indeed, solution NMR spectroscopy (vide supra) shows that the adduct is partially dissociated at this temperature.

In conclusion, the existence of the adduct **3** has been verified, both in solution and in the solid state. Calculated and experimentally determined thermodynamic data show that **3** is only weakly bound. Kinetic data indicate the presence of a dynamic equilibrium in THF solution. Theoretical and experimental studies to develop an understanding of the mechanism of the borylation of *α,β*-unsaturated ketones reported by Hoveyda et al. are the subject of ongoing research.

EXPERIMENTAL SECTION

Unless otherwise noted, all manipulations were performed using standard Schlenk or glovebox techniques under dry nitrogen. Reagent grade solvents were nitrogen saturated and were dried and deoxygenated using a solvent purification system and further deoxygenated by using the freeze−pump−thaw method. THF-d_8 was distilled from potassium/benzophenone followed by deoxygenation using the freeze−pump−thaw method. CyNHC was prepared according to a modification of the literature procedures.[16] B_2pin_2 was kindly provided by AllyChem Co. Ltd. (Dalian, China). All other commercial reagents were checked for purity by GCMS, elemental analyses, and/or NMR spectroscopy and used as received. They were, if appropriate, stored over thoroughly dried 4 Å molecular sieves. The solution state NMR spectra were recorded at ^{1}H 500 MHz, ^{13}C 125 MHz, ^{11}B 160 MHz or ^{1}H 400 MHz, ^{13}C 100 MHz, ^{31}P 162 MHz, ^{11}B 128 MHz. ^{1}H NMR chemical shifts are reported relative to TMS and were referenced via residual proton resonances of the corresponding deuterated solvent (THF-d_8 1.73, 3.58 ppm; MeCN-d_3 1.94 ppm; DMF-d_7 2.73, 2.91, 8.01 ppm), whereas ^{13}C NMR spectra are reported relative to TMS using the carbon signals of the deuterated solvent (THF-d_8 67.6, 25.4 ppm; MeCN-d_3 118.3, 1.3 ppm; DMF-d_7 30.1, 35.2, 162.7 ppm). The ^{11}B and ^{31}P NMR chemical shifts are reported relative to external $BF_3{\cdot}Et_2O$ and 85% H_3PO_4 in D_2O, respectively. All ^{13}C, ^{11}B, and ^{31}P NMR spectra were recorded with ^{1}H decoupling. Air sensitive NMR samples were handled under nitrogen using NMR tubes equipped with Teflon valves. The solid-state magic-angle spinning (MAS) NMR spectra were recorded at 128.30 MHz for ^{11}B and 100.56 MHz for ^{13}C (399.88 MHz for ^{1}H) using a 4 mm (rotor o. d.) MAS probe. The ^{11}B spectra were obtained using direct excitation with a 30° pulse and ^{1}H decoupling, with a 0.2 s recycle delay and at a spin-rate of 10 kHz. ^{11}B isotropic chemical shifts were estimated by simulating the observed spectrum using the Varian STARS program. Melting points were determined in flame-sealed capillaries filled with nitrogen.

B_2pin_2(CyNHC) (3). Under an atmosphere of nitrogen, **2** (65 mg, 280 *μ*mol) and **1** (71 mg, 280 *μ*mol) were mixed in dry toluene (2 mL). After 20 min, the mixture was concentrated to ca. 0.8 mL and left at −20 °C to crystallize. The mother liquor was decanted while cold (−20 °C), and the colorless, X-ray quality single crystals were washed with 5 mL of cold (−20 °C) *n*-hexane and dried in vacuo: mp 90−95 °C; *m*/*z* (EI) 486 (M^+), 471 $(M - CH_3)^+$, 422, 403 $(M - C_6H_{11})^+$, 359 $(M - Bpin)^+$, 345, 297, 254 $(B_2pin_2)^+$, 239, 155, 84; ^{1}H NMR (500 MHz; THF-d_8, 20 °C) *δ* 7.13 (br s, 2H), 5.49 (br s, 2H), 2.06 (br s, 4H), 1.79 (br s, 4H), 1.68 (br s, 2H), 1.50 (br s, 8H), 1.23 (br s, 2H), 1.00 (br s, 24H); ^{1}H (500 MHz; THF-d_8, 50 °C) *δ* 7.10 (s, 2H), 5.44 (br s, 2H), 2.08 (s, 4H), 1.84−1.76 (m, 4H), 1.73−1.67 (m (overlapping with THF signal), 2H), 1.51 (quint., *J* = 11 Hz, 8H), 1.28−1.16 (m, 2H), 1.02 (br s, 24H); ^{1}H NMR (500 MHz; THF-d_8, −10 °C) 7.19 (s, 2H), 5.49 (br s, 2H), 2.03 (br s, 4H), 1.86−1.63 (m (overlapping with THF signal), 6H), 1.56−1.43 (m, 8H), 1.28−1.16 (m, 2H), 1.01 (v br s, 24H); ^{1}H NMR (500 MHz; THF-d_8, −80 °C) 7.44 (s, 2H), 5.42 (t, *J* = 12 Hz, 2H), 2.00−1.96 (m, 4H), 1.79 (t, *J* = 12 Hz, 4H), 1.69 (d, *J* = 12 Hz, 2H), 1.62−1.39 (m, 8H), 1.26−1.14 (m, 2H), 1.04 (s, 12H), 1.03 (s, ov, 6H), 0.84 (s, 6H); ^{13}C{^{1}H} NMR (125 MHz; THF-d_8, RT) *δ* 169.3, 117.1, 79.7, 56.4, 34.7, 26.7, 26.5, 25.8; ^{13}C{^{1}H} NMR (125 MHz; THF-d_8, −85 °C) *δ* 167.5, 117.7, 83.6, 81.2, 55.8, 34.7, 34.4, 26.4, 26.3, 25.4; ^{11}B{^{1}H} NMR (160 MHz; THF-d_8, 50 °C) *δ* 20.4 (br); ^{11}B{^{1}H} NMR (160 MHz; THF-d_8, 20 °C) no signal detected (see text); ^{11}B{^{1}H} NMR (160 MHz; THF-d_8, 5 °C) *δ* 37.2 (v br s), 2.4 (br s); ^{11}B{^{1}H} NMR (160 MHz; THF-d_8, −85 °C) *δ* 1.5 (v br s); ^{13}C{^{1}H} solid-state NMR (100 MHz, RT) *δ* 168.4 (br), 119.4, 114.3, 80.9, 77.6, 56.4, 55.2, 35.3, 34.7, 33.8, 27.5, 27.0, 26.1, 25.1; ^{11}B{^{1}H} solid-state NMR (160 MHz, RT) *δ* 36, 2. Found: C, 66.96; H, 10.10; N, 6.10%. Calcd. for $C_{27}H_{48}O_4N_2B_2$ (**3**): C, 66.68; H, 9.95; N, 5.76%.

[*n*Bu_4P]$^+$ [$Bpin_2$]$^-$. Pinacol (3.00 g, 25.4 mmol, 2.0 equiv) and boric acid (0.75 g, 12.7 mmol, 1.0 equiv) were added to water (20 mL). After addition of [*n*Bu_4P]OH as a 40% aqueous solution (9.00 g, 12.7 mmol, 1.0 equiv), the mixture was stirred at 75 °C for 16 h. After removal of the solvent in vacuo, the residue was dissolved in THF (7 mL) and the solution extracted with *n*-hexane (2 × 10 mL). Upon standing, crystals separated from the THF layer, which were collected and recrystallized from hot THF/*n*-hexane to form crystals suitable for an X-ray diffraction study. The bulk material was dried in vacuo over P_4O_{10} for several days: mp 239−244 °C; *m*/*z* (ES^+) 259 $(nBu_4P)^+$, (ES^-) 243 $(Bpin_2)^-$; HRMS (ES^-) found 242.1827, calcd. for $(C_{12}H_{24}{}^{10}BO_4)$ 242.1804; found 243.1785, calcd. for $(C_{12}H_{24}{}^{11}BO_4)$ 243.1768; ^{1}H NMR (400 MHz; MeCN-d_3, RT) *δ* 2.08−2.00 (m, 8H), 1.54−1.39 (m, 16H), 0.94 (t, *J* = 8 Hz, 12H), 0.92 (s, 24H); ^{13}C{^{1}H} NMR (100 MHz; MeCN-d_3, RT) *δ* 77.1, 26.6, 24.9 (d, *J* = 15 Hz), 24.3 (d, *J* = 5 Hz), 19.4 (d, *J* = 48 Hz), 14.0 (d, *J* = 1 Hz); ^{31}P{^{1}H} NMR (162 MHz; MeCN-d_3, RT) *δ* 33.8 (s); ^{11}B{^{1}H} NMR (128 MHz; MeCN-d_3, RT) *δ* 8.6 (s); ^{11}B{^{1}H} NMR (128 MHz; THF-d_8, RT) *δ* 8.6 (s); ^{11}B{^{1}H} NMR (128 MHz; DMF-d_7, RT) *δ* 8.9 (s). Found: C, 67.29; H, 12.12; N, 0.00%. Calcd. for $C_{28}H_{60}O_4B$: C, 66.92; H, 12.03; N, 0.00%.

X-ray Crystallography. Single crystals coated with perfluoropolyether oil were each mounted on a human hair and cooled using an open-flow N_2 gas cryostat. A full sphere of data were collected on a diffractometer with a CCD detector (Mo K*α* radiation, *λ* = 0.71073 Å, *ω* scans, 0.3° wide) using the SMART[17a] software. The data were integrated using SAINT,[17b] and the structures were solved by direct methods and refined by full-matrix least-squares against F^2 of all data using SHELXTL programs.[17c,d] All non-hydrogen atoms were refined with anisotropic displacement parameters and hydrogen atoms were included in calculated positions and refined using a riding model. Analyses of the structures and the preparation of graphic were performed using ORTEP 3 and PLATON.[17e−g]

*X-ray data for B_2pin_2(CyNHC)·PhMe (**3**·PhMe).* $C_{34}H_{56}B_2N_2O_4$: M_r = 578.43, crystal size 0.46 × 0.34 × 0.22 mm^3, monoclinic, $P2_1/c$, *a* = 10.3682(3), *b* = 16.4505(5), *c* = 19.7145(7) Å, *β* = 91.028(1)°, *V* = 3362.0(2) Å^3, *Z* = 4, ρ_{calcd} = 1.143 g/cm^3, *μ* = 0.07 mm^{-1}, *T* = 120(2) K, $2\theta \leq 52.0°$, 32658 reflections with 6610 unique [*R*(int) = 0.104], *R*1= 0.041 (for 4582 unique data with $I > 2\sigma(I)$), *w*R2 = 0.105 (all data), max peak/hole = 0.25/−0.23 e$^-$/Å^3.

*X-ray Data for B_2pin_2 (**1**).* $C_{12}H_{24}B_2O_4$: M_r = 253.93, crystal size 0.8 × 0.7 × 0.3 mm^3, monoclinic, $P2_1/c$, *a* = 10.2834(3), *b* = 7.4809(5), *c* = 10.1672(8) Å, *β* = 110.48(1)°, *V* = 732.7(1) Å^3, *Z* = 2, ρ_{calcd} = 1.151 g/cm^3, *μ* = 0.081 mm^{-1}, *T* = 120(2) K, $2\theta \leq 60.0°$, 13019 reflections with 2143 unique [*R*(int) = 0.024], R_1= 0.040 (for 1842 unique data with $I > 2\sigma(I)$), wR_2 = 0.1194 (all data), max peak/hole = 0.41/−0.16 e$^-$/Å^3.

X-ray Data for [nBu_4P]$^+$ [$Bpin_2$]$^-$. $C_{28}H_{60}BO_4P$: M_r = 502.54, crystal size 0.38 × 0.16 × 0.12 mm^3, monoclinic, $P2/n$, *a* = 16.6584(4), *b* = 10.4920(2), *c* = 19.4579(4) Å, *β* = 112.753(1)°, *V* = 3136.2(1) Å^3, *Z* = 4, ρ_{calcd} = 1.064 g/cm^3, *μ* = 0.116 mm^{-1}, *T* = 120(2) K, $2\theta \leq$

dx.doi.org/10.1021/jo202127c | J. Org. Chem. 2012, 77, 785−789

52.0°, 40430 reflections with 6161 unique [R(int) = 0.0453], R_1= 0.041 (for 4667 unique data with $I > 2\sigma(I)$), wR_2 = 0.108 (all data), max peak/hole = 0.36/−0.25 e$^-$/Å^3. Crystallographic data for the structures reported in this paper have been deposited with the Cambridge Crystallographic Data Centre as supplementary publication No. CCDC 847767 to 847769. Copies of the data can be obtained free of charge on application to CCDC, 12 Union Road, Cambridge CB2 1EZ, U. K. Fax: +44(1223) 336-033; E-mail: deposit@ccdc.cam.ac.uk.

■ ASSOCIATED CONTENT

Supporting Information

Details of the NMR simulations, ^{13}C and ^{11}B solid-state NMR spectra, DFT computations, and crystal data. This material is available free of charge via the Internet at http://pubs.acs.org.

■ AUTHOR INFORMATION

Corresponding Author

*E-mail: paul.hodgkinson@durham.ac.uk (P.H.); chzlin@ust.hk (Z.L.); todd.marder@durham.ac.uk (T.B.M.).

■ ACKNOWLEDGMENTS

C.K. thanks the Deutsche Forschungsgemeinschaft (DFG) for a postdoctoral fellowship. T.B.M. thanks AllyChem Co. Ltd. for a generous gift of B_2pin_2, the Royal Society for a Wolfson Research Merit Award, the Alexander von Humboldt Foundation for a Research Award, EPSRC for an Overseas Research Travel Grant, and the Royal Society of Chemistry for a Journals Grant for International Authors. Z.L. thanks the Research Grants Council of Hong Kong for support (HKUST 603711). We thank the EPSRC National Solid-State NMR Research Service (Durham) for recording the solid-state NMR spectra and for valuable discussions, the EPSRC National Mass Spectrometry Service Centre (Swansea) for mass spectra, and J. Magee (Durham) for performing the elemental analyses.

■ REFERENCES

(1) (a) Haubold, W.; Hrebicek, J.; Sawitzki, G. *Z. Naturforsch.* **1984**, *39B*, 1027. (b) Nguyen, P.; Dai, C.; Taylor, N. J.; Power, W. P.; Marder, T. B.; Pickett, N. L.; Norman, N. C. *Inorg. Chem.* **1995**, *34*, 4290. (c) Clegg, W.; Dai, C.; Lawlor, F. J.; Marder, T. B.; Nguyen, P.; Norman, N. C.; Pickett, N. L.; Power, W. P.; Scott, A. J. *Dalton Trans.* **1997**, 839. (d) Grigsby, W. J.; Power, P. *Chem.—Eur. J.* **1997**, *3*, 368. (e) Kaufmann, B.; Jetzfellner, R.; Leissring, E.; Issleib, K.; Nöth, H.; Schmidt, M. *Chem. Ber./Recl.* **1997**, *130*, 1677.

(2) (a) Takahashi, K.; Ishiyama, T.; Miyaura, N. *J. Organomet. Chem.* **2001**, *625*, 47. (b) Bonet, A.; Gulyas, H.; Fernandez, E. *Angew. Chem., Int. Ed.* **2010**, *49*, 5130. (c) Bonet, A.; Pubill-Ulldemolins, C.; Bo, C.; Gulyás, H.; Fernández, E. *Angew. Chem., Int. Ed.* **2011**, *50*, 7158.

(3) (a) Gao, M.; Thorpe, S. B.; Santos, W. L. *Org. Lett.* **2009**, *11*, 3478. (b) Gao, M.; Thorpe, S. B.; Kleeberg, C.; Slebodnick, C.; Marder, T. B.; Santos, W. L. *J. Org. Chem.* **2011**, *76*, 3997.

(4) (a) Lee, K. S.; Zhugralin, A. R.; Hoveyda, A. H. *J. Am. Chem. Soc.* **2009**, *131*, 7253. (b) While our work was in progress, Hoveyda et al. published a very brief correction to their earlier report: Lee, K. S.; Zhugralin, A. R.; Hoveyda, A. H. *J. Am. Chem. Soc.* **2010**, *132*, 12766 (see also reference 3b).

(5) (a) Takahashi, K.; Ishiyama, T.; Miyaura, N. *Chem. Lett.* **2000**, 982. (b) Ito, H.; Yamanaka, H.; Tateiwa, J.; Hosomi, A. *Tetrahedron Lett.* **2000**, *41*, 6821. (c) Mun, S.; Lee, J.-E.; Yun, J. *Org. Lett.* **2006**, *8*, 4887. (d) Dang, L.; Lin, Z.; Marder, T. B. *Organometallics* **2008**, *27*, 4443. (e) Lillo, V.; Prieto, A.; Bonet, A.; Díaz-Requejo, M. M.; Ramírez, J.; Pérez, P. J.; Fernández, E. *Organometallics* **2009**, *28*, 659. (f) Sim, H.-S.; Feng, X.; Yun, J. *Chem.—Eur. J.* **2009**, *15*, 1939. (g) Lillo, V.; Bonet, A.; Fernández, E. *Dalton Trans.* **2009**, 2899. (h) Dang, L.; Lin, Z.; Marder, T. B. *Chem. Commun.* **2009**, 3987. (i) Schiffner, J. A.; Muether, K.; Oestreich, M. *Angew. Chem., Int. Ed.* **2010**, *49*, 1194. (j) Mantilli, L.; Mazet, C. *ChemCatChem* **2010**, *2*, 501. (k) Bonet, A.; Sole, C.; Gulyas, H.; Fernández, E. *Curr. Org. Chem.* **2010**, *14*, 2531.

(6) Kleeberg, C.; Apperley, D.; Mo, F.; Qiu, D.; Cheung, M. S.; Dang, L.; Wang, J.; Lin, Z.; Marder T. B. manuscript in preparation; Presented in part at IMEBORON XIV, Niagara Falls, Canada, September 2011.

(7) Nöth, H.; Wrackmeyer, B. *NMR Basic Princ. Prog.* **1978**, *14*, 1.

(8) (a) Nöth, H. *Z. Naturforsch., B: J. Chem. Sci.* **1984**, *39*, 1463. (b) Dang, L.; Zhao, H.; Lin, Z. Y.; Marder, T. B. *Organometallics* **2008**, *27*, 1178.

(9) See Supporting Information for details.

(10) Kleeberg, C.; Dang, L.; Lin, Z.; Marder, T. B. *Angew. Chem., Int. Ed.* **2009**, *41*, 5350.

(11) Yamaguchi, Y.; Kashiwabara, T.; Ogata, K.; Miura, Y.; Nakamura, Y.; Kobayashi, K.; Ito, T. *Chem. Commun.* **2004**, 2160.

(12) For selected NHC−B-adducts see: (a) Arduengo, A. J., III; Davidson, F.; Krafczyk, R.; Marshall, W. J.; Schmutzler, R. *Monatsh. Chem.* **2000**, *131*, 251. (b) Phillips, A. D.; Power, P. P. *Acta Crystallogr.* **2005**, *C61*, o291. (c) Solovyev, A.; Chu, Q.; Geib, S. J.; Fensterbank, L.; Malacria, M.; Lacote, E.; Curran, D. P. *J. Am. Chem. Soc.* **2010**, *132*, 15072. (d) Braunschweig, H.; Chiu, C.; Radacki, K.; Kupfer, T. *Angew. Chem., Int. Ed.* **2010**, *49*, 2041. (e) Holschumacher, D.; Bannenberg, T.; Hrib, C. G.; Jones, P. G.; Tamm, M. *Angew. Chem., Int. Ed.* **2008**, *47*, 7428. (f) Kinjo, R.; Donnadieu, B.; Celik, M. A.; Frenking, G.; Bertrand, G. *Science* **2011**, *333*, 610. (g) Bissinger, P.; Braunschweig, H.; Kraft, K.; Kupfer, T. *Angew. Chem., Int. Ed.* **2011**, *50*, 4704. (h) Bissinger, P.; Braunschweig, H.; Damme, A.; Dewhurst, R. D.; Kupfer, T.; Radacki, K.; Wagner, K. *J. Am. Chem. Soc.* **2011**, No. DOI: 10.1021/ja208372k.

(13) The purities of the samples of isolated **3** used for NMR experiments were verified by elemental analyses. Furthermore, a solid-state ^{13}C NMR spectrum confirmed the purity and identity of one sample.

(14) (a) Dale, J. *J. Chem. Soc.* **1961**, 922. (b) Kalacheva, V. G.; Svarcs, E.; Benkovskii, V. G.; Leonov, I. D. *Zh. Neorg. Kh.* **1970**, *15*, 401. (c) Henderson, W. G.; How, M. J.; Kennedy, G. R.; Mooney, E. F. *Carbohydr. Res.* **1973**, *28*, 1.

(15) (a) Sandström, J. *Dynamic NMR Spectroscopy*; Academic Press Inc.: London, 1982; Chapter 7. (b) Jackman, L. M.; Cotton, F. A. *Dynamic Nuclear Magnetic Resonance Spectroscopy*; Academic Press Inc.: New York, 1975.

(16) (a) Arduengo, A. J.; Dias, H. V. R.; Harlow, R. L.; Kline, M. *J. Am. Chem. Soc.* **1992**, *114*, 5530. (b) Herrmann, W. A.; Kocher, C.; Gooßen, L. J.; Artus, G. R. J. *Chem.—Eur. J.* **1996**, *3*, 1627.

(17) (a) *SMART 5.625*; Bruker AXS, Inc.: Madison, WI, 2001. (b) *SAINT 6.45*; Bruker AXS, Inc.: Madison, WI, 2003. (c) Sheldrick, G. M. *SHELXTL 6.14*; Bruker AXS, Inc.: Madison, WI, 2003. (d) Sheldrick, G. M. *Acta Crystallogr.* **2008**, *A64*, 112. (e) Farrugia, L. J. *J. Appl. Crystallogr.* **1997**, *30*, 565. (f) Spek, A. L. *Acta Crystallogr.* **1990**, *A46*, C34. (g) Spek, A. L. *PLATON, A Multipurpose Crystallographic Tool*; Utrecht University: Utrecht, The Netherlands, 1998.